Imperial College London

The Use of Non-invasive Techniques for the Early Detection of Pressure Ulcers

Dr Fernando Bello (Supervisor)
Reader in Surgical Graphics and Computing

Chelsea & Westminster Hospital
3rd Floor – Academic Department of Surgery & Cancer
Chelsea and Westminster Hospital
369 Fulham Rd
London SW10 9NH
f.bello@imperial.ac.uk

Word Count: 4,450

Mohammed Umar Riyaz CID: 00685088

Abstract

Aim The ultimate aim of this project is to develop a non-invasive image-based erythema detection device to assist medical professionals in detecting pressure ulcers in their very early stages.

Background Described as ‘a silent epidemic’, pressure ulcers pose a substantial challenge to health services. 4-10% of patients admitted to UK hospitals incur pressure ulcers during their stay. Financial costs to the NHS are estimated to be between £1.4 billion - £2.1 billion annually. With an aging population, incidence is likely to increase. There is a high demand to develop a device to assist healthcare professionals in detecting pressure ulcers. Earlier detection is associated with reduced mortality.

Method Following skin indentation, reactive hyperaemia was induced in the left and right forearm of twelve subjects. The indented area of the left arm was imaged, and right arm videoed. The images were enhanced through linear normalisation, global histogram equalisation and contrast limited adaptive histogram equalisation (CLAHE). The videos were processed through eularian colour magnification. The efficacy was assessed through comparison in luminance values and feedback from tissue viability specialists.

Results These preliminary findings have confirmed that image processing can be used to improve image contrast and subsequently aid in the detection of erythema. This applies to all skin colours. This is the first time eulerian colour magnification has

been applied to detect skin pathology. Initial samples suggest immense potential.

Conclusion In the absence of any gold standard pressure-ulcer detection method, this is a first step in developing an innovative non-invasive erythema detection device.

Background

Pressure ulcers (PU) have been defined as an area of localised damage to the skin and underlying tissue caused by pressure, shear, friction or a combination of these factors (European Pressure Ulcer Advisory Panel).[1]

When standing, sitting or lying, skin, subcutaneous fat and muscle are compressed between bone and an external surface. In the distorted tissue, blood vessels are compressed, stretched out or angulated, causing microvascular occlusion.[2] The tissues supplied by those blood vessels can become hypoxic and mildly ischaemic. In healthy individuals, discomfort is felt, and the body position is adjusted to relieve the pressure. Following reactive hyperaemia, the ischaemia and hypoxia resolve leading to no long term pathology.[3]

If the pressure is sustained, metabolic waste products, proteins and enzymes can accumulate, leading to necrosis, and an inflammatory response.[4] Even when the occluding pressure is removed, the individual is likely to suffer from reperfusion injury.[5] This localised injury is known as a pressure ulcer. Subsequent infection is a major concern. Bony prominences, such as the sacrum, heels and the back of the skull are at greatest risk.[6]

Described as ‘a silent epidemic’, pressure ulcers pose a substantial challenge to health services.[7] 4-10% of patients admitted to UK hospitals incur pressure ulcers during their stay.[8] There are substantial financial costs to the NHS, estimated to be between £1.4 billion - £2.1 billion annually.[9] Treatment of cases vary from £1,064

(Grade 1) to £10,551 (Grade 4).[8] Due to changing age demographics involving an aging population, this cost is likely to increase in future.

Litigation and reimbursement disputes augment the burden of pressure ulcers. Pressure damage may be viewed as evidence of clinical negligence.[10] Though the threat of litigation in the UK is currently incomparable to the USA, there is evidence to suggest it is increasing. To avoid litigious repercussions, documenting pressure ulcers “present on admission” has become a priority in the USA. As of October 2008, reimbursements for nosocomial pressure ulcers costs are no longer provided by The Centers for Medicare and Medicaid Services (CMS).[11]

Pressure ulcers are associated with increased morbidity and mortality. From October 1997 to October 2002, a non-experimental, retrospective analysis of pressure ulcer quality assurance data was conducted to determine the relationship between nosocomial full-thickness pressure ulcers, healing, and mortality. It found that of those who sustained full-thickness pressure ulcers, 68.9% died within 180 days.[12] Although this correlation does not necessitate causation, it does emphasise that severe pressure ulcers and death are common co-occurrences. This observation has been highlighted by the Skin Changes at Life’s End Expert Panel in a consensus statement.[13]

It is therefore of critical importance that measures are taken to prevent pressure ulcer formation. This begins by Identifying patients considered to be at an increased risk. Risk factors include lack of sensory perception (inability to detect discomfort indicating potential ulcer), paralysis (inability to relieve pressure), excessive skin

moisture or dryness (increased friction) and smoking (reduced blood flow and limited oxygen saturation).[14] Tools have been developed to identify these risk factors, such as the Braden Scale and the Waterlow Score. However, their efficacy has been questioned.[15]

Preventing pressure ulcers also relies on labour-intensive vigilance by nurses.[16] Patients must regularly be manually repositioned to relieve pressure. Hard surfaces result in high pressures at the bone-tissue interface and increase pressure ulcer risk.[17] Staff in operating theatres, accident and emergency, and radiology must be particularly attentive.[18] Additional use of air products, gel or polymer may reduce risk.

High-risk regions are visually inspected[16]. Circular red regions of blanching erythema over bony prominences may indicate pressure damage.[19] If pressure is sustained, the discolouration will further darken.[1] In patients with darker skin shades, the discolouration is more difficult to spot and does not blanch white, increasing their risk of developing a pressure ulcer.[20]

Currently, visual inspection constitutes a highly subjective and unreliable way of classifying pressure ulcers. This has been demonstrated by inter-observer reliability studies which highlighted discrepancies in stage analysis. Non-blanchable erythema was frequently assessed incorrectly as blanchable erythema. The studies emphasise the need for unambiguous definitions and descriptions.[21]

Early detection of pressure ulcers is critical to reducing pain, mortality and treatment costs. Currently, no reliable method exists to detect pressure induced early tissue

damage, though multiple attempts have been made.

Attempts at Identifying general skin wounds can be grouped into two categories: Visual assessment apparatuses, which involve colour and digital image analysis, and physiological-based apparatuses involving pressure measurements, blood flow or force. In 2008, Weber et al.[22]begun developing an electrical impedance device to help determine the severity of a wound using the tissues' electrical characteristics. Treuillet et al. have developed a novel approach to construct 3D models of skin wounds using uncalibrated images captured with a handheld digital camera.[23] Though this could be useful for assessing wound surface, depth, or volume, it is not applicable to early pressure ulcer formation where the skin has not been deformed.

Attempts at developing techniques for the detection of pressure ulcers are less numerous. One approach has been to exploit the elastic properties of the pressure ulcer. In some ulcers a gradual stiffening arises from the deeper tissues and progresses towards the skin. Ultrasound elastography maps these changes. In 2007, a cryogel phantom mimicking an early stage pressure ulcer was designed. An algorithm was developed, and applied to the ultrasound signal. This was able to detect a subepidermal layer, helping to differentiate between pathological and healthy regions. The course resolution and the unrealistic nature of the phantom were limitations.[24] In 2011, this method was repeated in animal studies with promising results. Human trials are yet to be conducted.[25]

In March 2015, a non-invasive, flexible, impedance spectroscopy device that maps pressure-induced tissue damage was announced. In damaged cells, the membrane

loses structure and integrity, allowing ions and current to travel through the membrane. The ‘smart bandage’ exploits these surface electrical conductance variations to expose pathology. Currently trials have been limited to rat models.[27]

Significant research has been published exploring image processing for wound diagnosis. Diverse segmentation methods, such as watersheds, mean-shift smoothing, histogram thresholding, and region growing have been employed to detect the varied tissues in a wound.[28]

More pertinently, other approaches have focussed on wound identification. Active contours modelling, histogram segmentation, region growing, clustering approaches and skin texture models have been explored.[29]

In the context of pressure ulcer detection, a multispectral imaging device prototype that fabricates and integrates filter mosaic with commercial imaging sensors has been developed. Hairong Qi et al. attempted to overcome filter misalignment and missing spectral components which hindered practical deployment of the device. It has yet to reach the market.[30]

Rajendran P.J. et al. have explored image histogram manipulation to improve the contrast of indented sites. These sites were intended to mimic erythema present prior to pressure ulcer formation. Though the study showed promising results, it was not validated by clinicians, nor had it been trialled on patients.

As elucidated, there is a necessity to translate these pilot studies into a validated

functional device. The ultimate aim of this project is to develop a non-invasive image-based erythema detection device to assist medical professionals in detecting pressure ulcers in their very early stages. This will improve prognosis and reduce healthcare costs. This paper presents the preliminary results of enhancing images and video to improve erythema visualisation.

Method

Following skin indentation, reactive hyperaemia was induced in the left and right forearm of twelve subjects. The indented area of the left arm was imaged, and right arm videoed. The images were enhanced through linear normalisation, global histogram equalisation (GHE) and contrast limited adaptive histogram equalisation (CLAHE). The videos were processed through eularian colour magnification. The efficacy was assessed through comparison in luminance values and feedback from tissue viability specialists.

A. Subjects

12 subjects were recruited based on skin colour. They were categorised as black, brown, and white. Four subjects were assigned to each category. 8 of the subjects were male and 4 were female.

Subjects with a history of skin conditions or tattoos were excluded. All subjects provided verbal informed consent. The indentation and imaging took 30 minutes per participant. The experimental protocol was approved by the Academic Department of Surgery & Cancer of Chelsea and Westminster Hospital NHS Trust.

B. Indenting Procedure

A 12mm steel sphere was placed in a cavity and mounted on a platform. For a period of 2 minutes, subjects positioned the medial aspect of their left forearm on the

sphere, 60mm distal to their antecubital fossa. Indentation pressure was delivered by the weight of the arm, estimated as 50 mmHg. Following the removal of the indentation pressure, the medial aspect of the left forearm was imaged, and subsequently re-imaged at 30 second intervals for 5 minutes. The same procedure was performed on the right forearm, but videoed for five minutes once the indentation pressure had been removed.

C. Imaging Procedure

A digital single lens-reflex digital camera (20.2 megapixel CMOS sensor with a spectral range of 380nm to 750nm) was used to capture the images and video. Light was provided by overhead incandescent bulbs and frontal light emitting diodes. Flash was not used. Exposure was set to maintain a high dynamic range and avoid loss of detail. The camera was positioned 0.5m from indented area, capturing an area encompassing the antecubital fossa and the tips of the fingers. Images were attained in the JPEG file format with a compression ratio of 5:1, resulting in a negligible loss of image quality[32].

The indented area of the right arm was videoed for five minutes with a resolultion of 1080p 25fps the same camera and with a fixed exposure. It was recorded in the H.264 MPEG-4 file compression format.

D. Image Enhancement

The images were normalised by linearly stretching the histogram. This improved the contrast by spreading the pertinent data across a greater range. 2% of data at the high intensity were saturated, with no saturation at the lower intensities. This was to prevent losing critical information in the darker regions.

To further enhance detail, the global histogram equalisation (GHE) algorithm was applied. This is a monotonic, non-linear reassignment of intensity values to generate a uniform distribution. The most frequent intensity values are spread out. This function is particularly advantageous when pertinent data are of close contrast values. A drawback of this algorithm is that it is indiscriminate, equally handling all regions, regardless of their relevance. The contrast of the background noise may be heightened and the signal of the indented area may be suppressed. This yields inadequate local performance.

Given this circumstance, an algorithm that enhanced local contrast was required. Adaptive histogram equalisation (AHE) divides an image into square domains and computes separate histograms for each domain. The histograms are then equalised to normal distribution. To prevent harsh transitions between domain boundaries, the blocks are re-joined using bilinear interpolation. The block size was set to 300*300 pixels to match the size of indented area.

A variant of AHE, contrast limited adaptive histogram equalisation (CLAHE) was employed. This limits contrast enhancement by clipping the histogram at a defined

value prior to calculating the cumulative distribution function. The benefit of this is the inhibition of an over amplification of noise.

E. Video Enhancement

Eularian colour magnification was applied to the video through the open-source software developed by Frédo Durand et. al from the Massachusetts Institute of Technology. This video processing technique can amplify subtle temporal colour changes that cannot be perceived by the naked eye. It works by applying spatial decomposition and temporal filtering to the video frames, and subsequently a magnification factor to amplify the removed band-pass signal. If applied correctly, this algorithm allows the user to visualise subtle variations on the skin.[33]

F. Luminance Values

The improvement between the original and the enhanced images were measured by comparing luminance values. Firstly, to gage the change in contrast of the indented area against the original skin shade, a 20*20 pixel square sample was taken from the indented area and five control areas of surrounding unaffected skin. The average pixel luminance of the indented area (L_i*) and control samples (L_c*) were recorded. The mean luminance of the control samples was then calculated (L_c**). Then, the luminance difference ($\triangle L^*_{\text{pre-enhancement}}$) between the indented area and control were calculated through subtraction (L_c**-L_i*). This was done for all 12 of the original images.

Following this, the same samples were taken and calculations were performed but on the image post-enhancement ($\triangle L^*_{post\text{-}enhancement}$). To compare the degree by which the enhancement made the indentation more visible, the enhancement ratio ($\triangle L^*_{ratio}$) was calculated by dividing $\triangle L^*_{post\text{-}enhancement}$ by $\triangle L^*_{pre\text{-}enhancement}$.

$$\triangle L^*_{ratio} = \triangle L^*_{post\text{-}enhancement} \Big/ \triangle L^*_{pre\text{-}enhancement}$$

G. Questionnaire

To further validate and refine the image enhancement techniques, a questionnaire was filled out by 10 medical professionals. Respondents were shown images pre-enhancement and post-enhancement and respondents were asked whether they could spot any abnormality. If they could they were asked to state how clear this was on a scale of 1-10. The nature of the abnormality was not enumerated to avoid biasing results. Respondents were then shown 30 images consisting of 10 variations of 3 subjects. The variations were of different block-size domains. Respondents were asked to mark which variation made the abnormality most clear.

Results

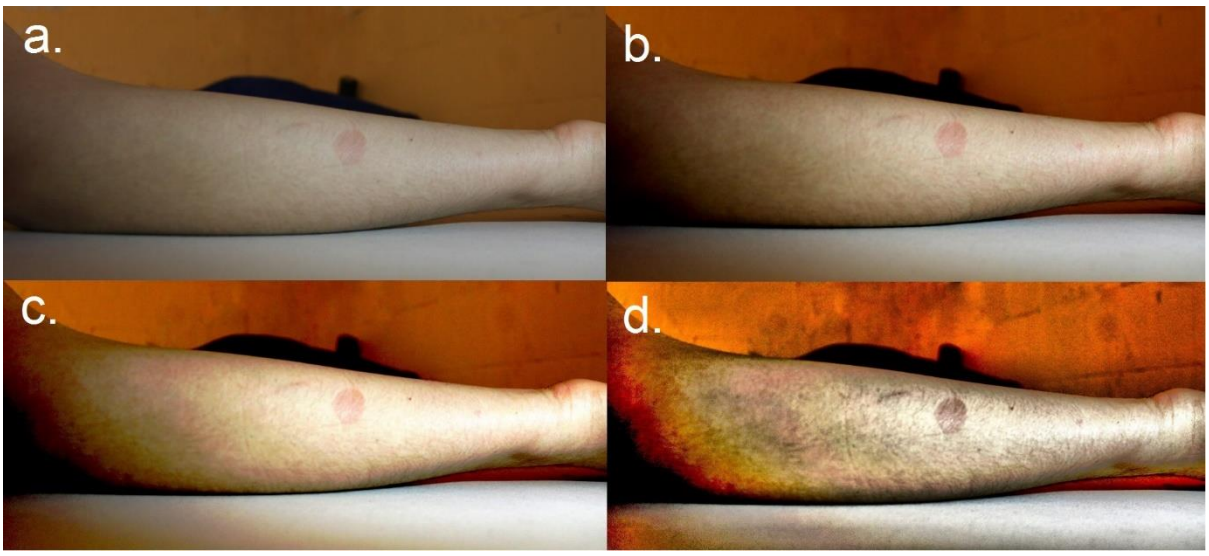

Figure. 1 shows (a) the pre-processed image, (b) the linearly normalised image, (c) the global histogram equalisation image, and (d) the contrast limited adaptive histogram equalised (CLAHE) image of the post indented medial aspect of the left forearm. This subject was categorised in the white skin colour category.

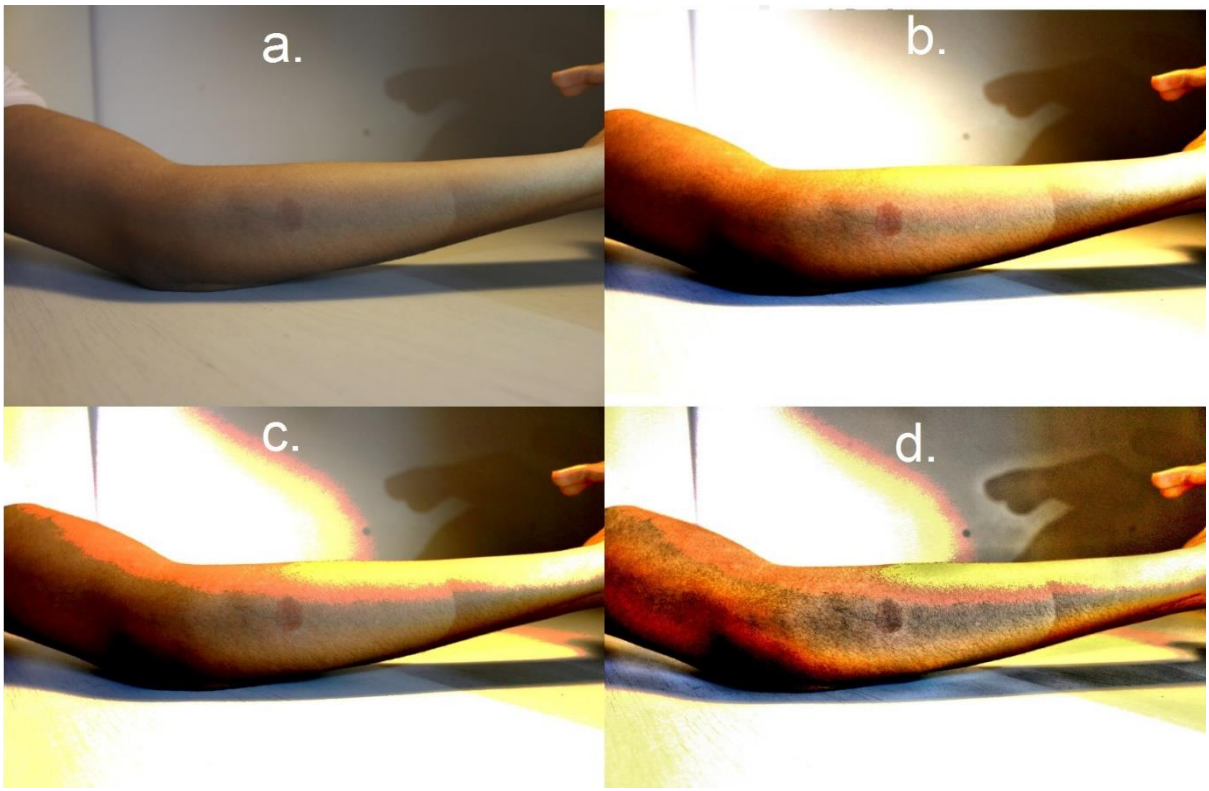

Figure. 2 shows (a) the pre-processed image, (b) the linearly normalised image, (c) the global histogram equalisation image, and (d) the contrast limited adaptive histogram equalised (CLAHE) image of the post indented medial aspect of the left forearm. This subject was categorised in the brown skin colour category.

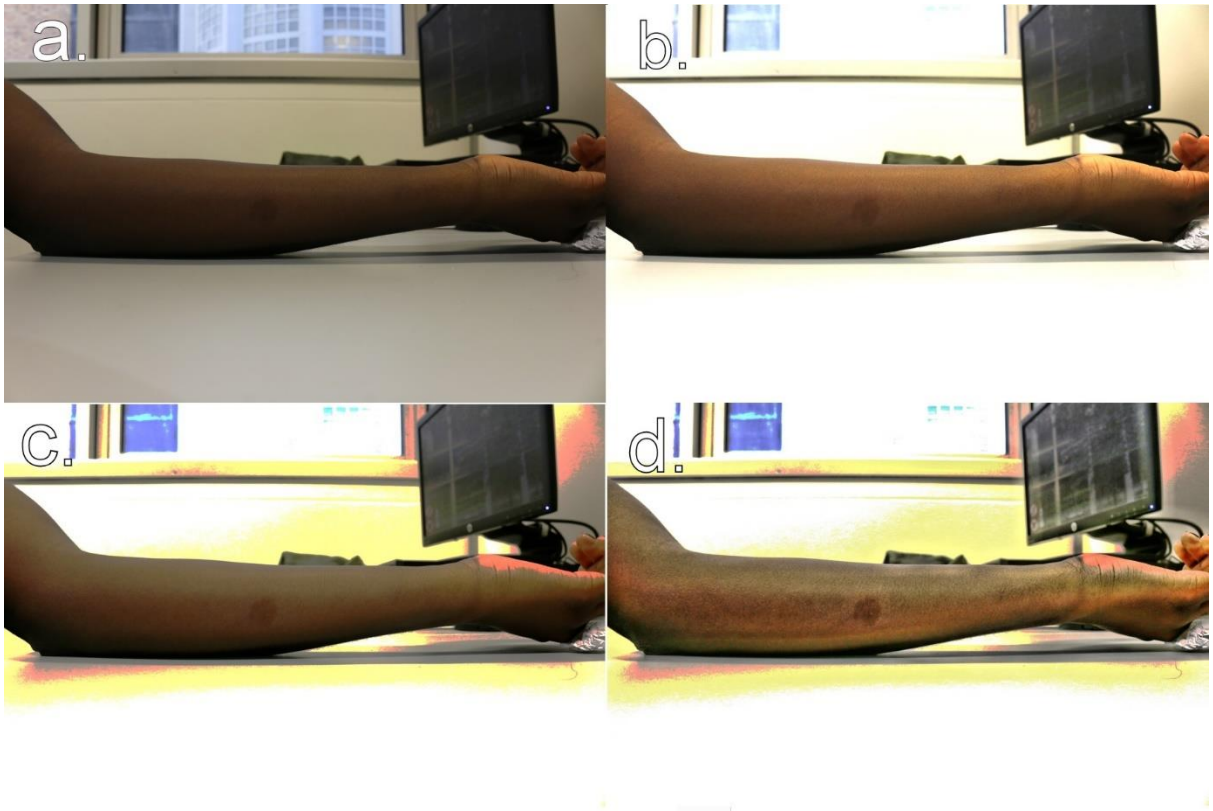

Figure. 3 shows (a) the pre-processed image, (b) the linearly normalised image, (c) the global histogram equalisation image, and (d) the contrast limited adaptive histogram equalised (CLAHE) image of the post indented medial aspect of the left forearm. This subject was categorised in the black skin colour category.

Sample	Mean $\triangle L^*_{pre\text{-}enhancement}$	Mean $\triangle L^*_{post\text{-}enhancement}$	$\triangle L^*_{ratio}$
White Skin	10.02	36.12	3.60
Brown Skin	11.8	43.02	3.65
Black Skin	8.44	32.85	3.89

Table I shows the Mean $\triangle L^*_{pre\text{-}enhancement}$, $\triangle L^*_{post\text{-}enhancement}$, and the $\triangle L^*_{ratio}$ for all the subjects that took part in the study.

A t-test for means was used to compare the $\triangle L^*_{pre\text{-}enhancement}$ and $\triangle L^*_{post\text{-}enhancement}$ for each of the four images in the three categories. The test showed that the level of enhancement of the images, represented by the $\triangle L^*_{ratio}$ was statistically significant for every skin colour category. The two-tailed test yielded a p value <. 0001 for all the images compared.

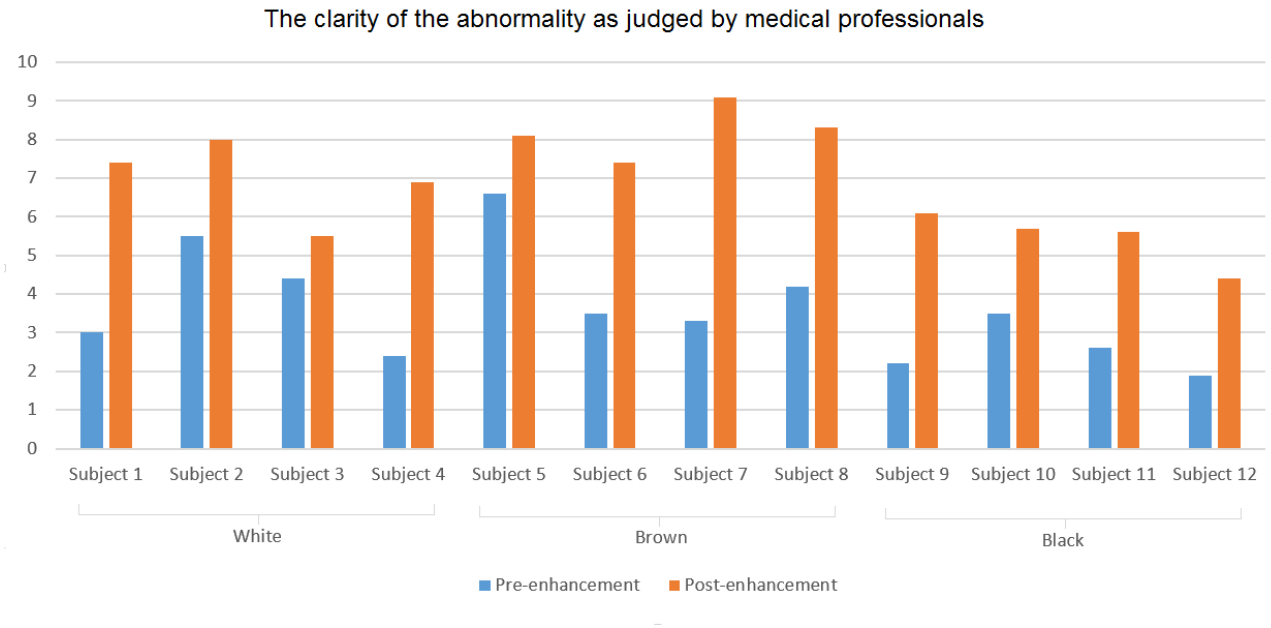

Figure 4. A bar chart representing the mean rating of the clarity of the abnormality by ten medical professionals. The blue bar represents the mean score pre-enhancement and the orange bar is the mean score post-enhancement. Subjects 1-4 were classed in the white skin category. Subjects 5-8 were classed in the brown skin category. Subjects 9-12 were classed in the black category. The improvement that the enhancement gave to each image is represented by the difference between the two adjacent bars of each subject. Those who were unable to detect any abnormality were assigned a score of 0.

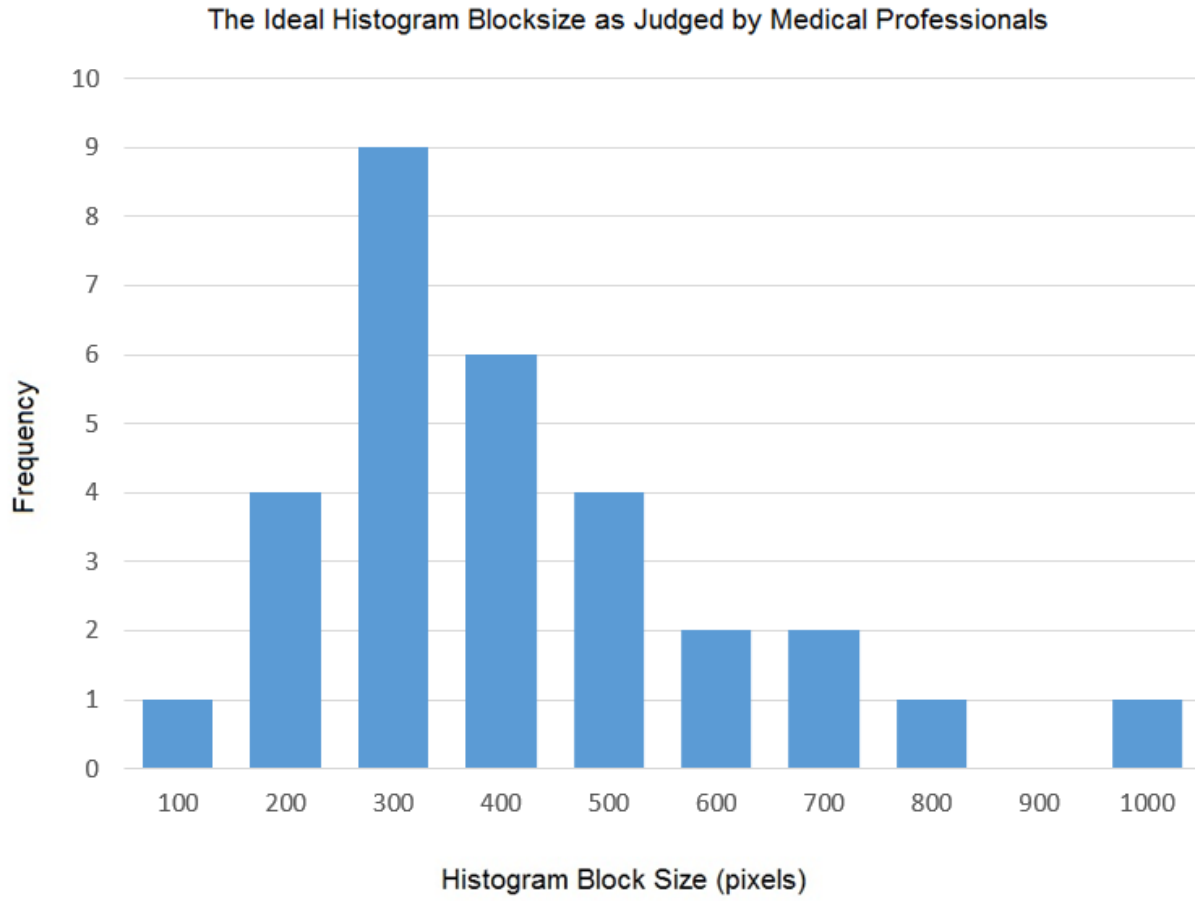

Figure 5. This bar chart represents the ideal histogram block-size of ten medical professionals. The most frequently chosen block-size was 300*300 pixels. The data did not follow a normal distribution.

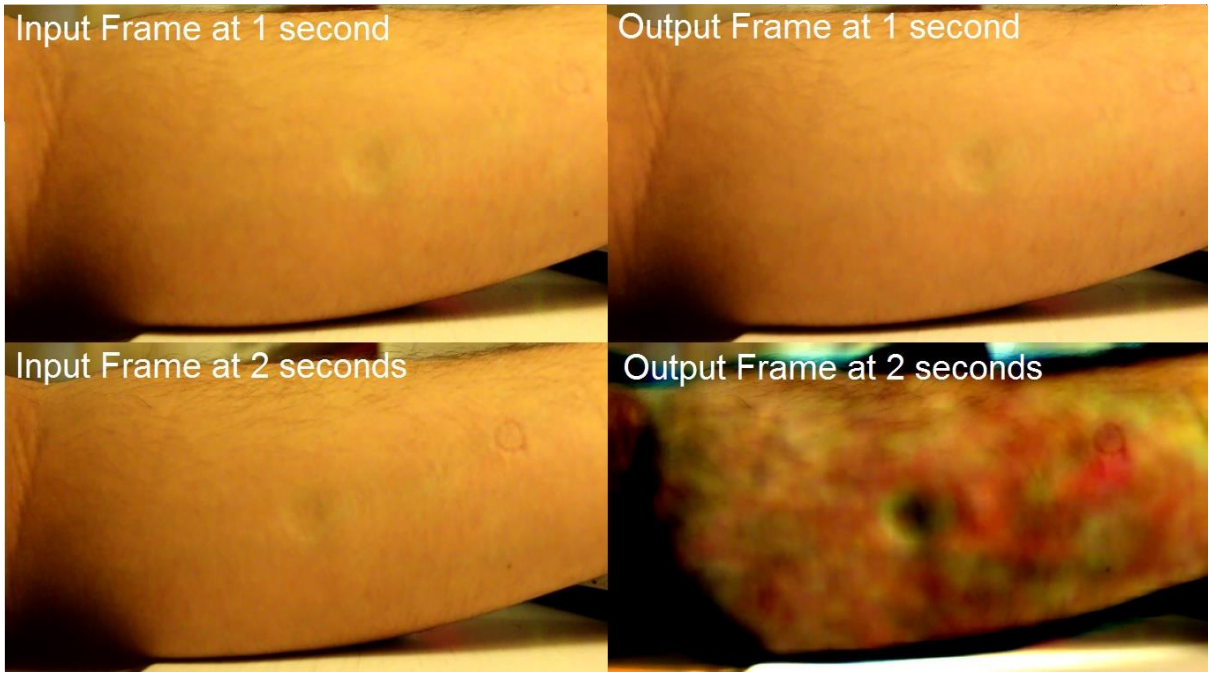

Figure 6. shows frames pre- and post- Eulerian Colour Magnification. The top left image is a screenshot of a frame at second 1. The top right is same frame but after Eulerian processing. The bottom left image is a screenshot of a frame at second 2. The bottom right image is same frame but after Eulerian processing. The variation due to the pulse has been magnified. When the pulse of the blood reaches a certain spot, the skin in that region will get darker.

Discussion

As can be seen in Figures 1, 2 and 3, the overall image enhancements improved the visual clarity of the indented area. It was observed that the global histogram equalisation function did not always enhance the image. This is perhaps best demonstrated between Figures 1b and 1c where the global histogram equalisation caused an over-exposure in the region of interest. Though this was somewhat counteracted by the adaptive histogram function (Figure 1d), the saturation effect lingered.

Manipulating the contrast through the linear stretching of the histogram yielded the most reliable results. In all subjects, this visibly improved contrast, with minimal artefacts. The contrast limited adaptive histogram equalisation function (CLAHE), was best at highlighting inconspicuous details. This is demonstrated in Figure 1d where a mark 1cm proximal to the indentation can be made out. In Figure 2d, marks in the elbow region can be envisaged.

The luminance tool calculates the grayscale value for a select area, providing separate weighting to R, G, and B inputs. Luminance comparisons were made to assess the degree of contrast. This was decided as the visual system distinguishes entities based on contrast, as opposed to absolute luminance.

It was imperative to select samples from all sides of the indented region as light often fell unevenly across the forearm. To prevent skewed calculations, an average of the samples was taken. Through luminance measurements (Table 1), it was theoretically

proven that the image processing functions enhanced the image.

The Mean $\triangle L^*_{pre\text{-}enhancement}$ column in Figure 1 hinted that the original indentation was more difficult to see in black subjects (8.44) than brown (11.88) and white (10.02) subjects. This difference was statistically significant to a 95% confidence level. The reason for this difference is that erythema is masked in darker skinned individuals by higher levels of melanin in the skin. This discrepancy has been manifest in clinical practice. In a study Rosen et al. showed that in nursing homes, no grade 1 pressure ulcers (non-blanching erythema) were documented in black residents, yet 31.6% of pressure ulcers in white residents were classed as grade 1.[34] Nixon et al. emphasised that failure to recognise non-blanching erythema is a risk factor for developing more severe forms of pressure ulcers.[35] Lyder C. et al. reported that twice the number of black patients developed Stage III and IV pressure ulcers than white patients.

Post-enhancement, the indentation in the brown skin category was most visible with the highest Mean $\triangle L^*_{post\text{-}enhancement}$ value (43.02). The white skin category was next most visible (36.12) and the black skin category was third (32.85). Unsurprisingly, this order mirrors the pre-enhancement order. This means that the already-most visible indentation remains most visible after image processing and vice-versa. It must be noted that the Mean $\triangle L^*_{post\text{-}enhancement}$ value of 32.85 for the black skin category is still an improvement which greatly improves detection ability.

The comparison between the Mean $\triangle L^*_{pre\text{-}enhancement}$ and Mean $\triangle L^*_{post\text{-}enhancement}$ was represented by the $\triangle L^*_{ratio}$ column. The black skin category had the greatest

improvement due to the image enhancement with a $\triangle L^*_{ratio}$ of 3.89. A t-test for means was used to for each of the three categories. The test showed that the degree of enhancement of the images, represented by the $\triangle L^*_{ratio}$ was statistically significant for every category, yielding a p value <. 0001 in the two-tailed t-tests. This implies that this image enhancement technique is highly reliable.

Figure 4 represents the subjective analysis of the pre- and post-enhancement images by 10 medical professionals. The findings echo the order of the luminosity analysis. The highest pre-enhancement average was of the brown category (4.4), followed by the white category (3.78) and then then black category (2.48). The same order exists post-enhancement. The highest post-enhancement average was of the brown category (8.18), followed by the white category (6.93) and then then black category (5.43). The improvements in average listed the brown skin type highest (3.78), followed by white (3.15) and then black (2.95). Improvements can also be calculated as a fraction, which would place the black skin type as the most improved (2.1), followed by brown (1.86), and then white (1.83). Due to the arbitrary nature of the scale, these inferences must be viewed in context.

The histogram block-size is the size of the local region around a pixel for which the histogram is equalised, measured in pixels. Figure 5 reveals that block-size that produces the most conspicuous indentation area is of 300*300 pixels. This is the same size as the area of indentation. We learn that the histogram block-size should be proportional to the area of interest. As the distance of the forearm to the camera was largely controlled, it is expected that most of the images would fall in the same range. However, occasionally a subject would tilt their arm, producing an ovular and

hence larger indentation size. Additionally some subjects did not provide adequate pressure, resulting in a smaller indentation size. This partially explains some of the variation. The question did rely on human subjective interpretation, and the differences between the varying images were slender, further explaining the variation. The data did not follow a normal distribution due to the squaring of the pixel width resulting in a disproportional output. The ideal histogram block-size can only be applied if the user is aware of the size of the entity being identified. In the case of pressure ulcer detection, where one is unaware of the size of the damage, estimates will have to be applied.

Figure 6 reveals the immense potential of eulerian colour magnification to detect early stage pressure ulcers. The software exaggerates minute changes in the skin colour. The method induced reactive hyperaemia, which involved a transient increase in blood flow to the affected area. This was detected by the camera, and exaggerated through the software. The output frame at 2 seconds demonstrates the extent to which details can be exposed. The indentation is significantly more pronounced and blood vessels can be seen. This technique does what image editing cannot do, as it exploits temporal variations in colour.

Limitations

Despite the promising results, some limitations exist. While the theoretical and applied measures indicated that the area could more easily be visualised, this comes at a cost. High amounts of noise make it more difficult to correctly distinguish true from false pathology. False positive findings can lead to unnecessary anxiety and

increased healthcare costs.

Additionally, some enhancement methods need to be tailored to the individual patient. When linearly stretching the contrast it advisable to saturate data from darker regions in light-skinned patients, and saturate data from the light intensities in dark skinned patients. To overcome this, the original skin colour must be manually inputted or automatically detected before the adjustment of contrast. When applying the global histogram equalisation function, one must be vigilant regarding background colours, as this can skew editing against the intended purpose.

Furthermore, this study used a steel ball to induce indentation. This led to a spherical region of reactive hyperaemia. However, in patients pressure ulcers usually have irregular shapes, vague boundaries and heterogeneous colourations. The medial aspect of the forearm was chosen as the area of indention. This has relatively little hair and few creases, whereas the back of the heels and elbows are relatively common sites for pressure ulcers. The skin in these regions are coarse and vary in colour, making pressure ulcers more difficult to detect.

Whilst much can be inferred from the varying responses to erythema in the different skin types, it must be noted that some of these differences may be due to other factors. It was observed that one of the patients in the white skin category was overweight, so the indented region was subsequently blurred. Moreover, the subjects in the brown skin types tended to be leaner. In future studies of this nature, the BMI of subjects must be controlled. Also, variations in indentation pressure existed as the weight of the arm of the subject was used to provide the pressure.

Conclusion

In the absence of any gold standard pressure-ulcer detection method, this is a first step in developing an innovative non-invasive erythema detection device. These preliminary findings have confirmed that image processing can be used to improve image contrast and subsequently aid in the detection of erythema. This applies to all skin colours. The image processing techniques elucidated in this paper can be adapted to the characteristics of the patients.

This is also the first time eulerian colour magnification has been applied to detect skin pathology. Initial samples suggest immense potential.

Future studies should focus on validating these findings in patients and integrating image processing techniques with ultrasound elastography and impedance spectroscopy.

References

1. European Pressure Ulcer Advisory Panel and National Pressure Ulcer Advisory Panel. Prevention and treatment of pressure ulcers: quick reference guide. Washington DC: National Pressure Ulcer Advisory Panel. 2009.

2. Roe E, Williams DL. Using evidence-based practice to prevent hospital-acquired pressure ulcers and promote wound healing. Am J Nurs. 2014 Aug;114(8):61-5.

3. Gillespie BM, Chaboyer WP, McInnes E, Kent B, Whitty JA, Thalib L. Repositioning for pressure ulcer prevention in adults. Cochrane Database of Systematic Reviews. 2014; Issue 4.

4. Farid KJ, Winkelman C, Rizkala A, Jones K. Using temperature of pressure-related intact discolored areas of skin to detect deep tissue injury: an observational, retrospective, correlational study. Ostomy Wound Manage. 2012 Aug; 58(8) 20-31. PMID: 22879313.

5. Peirce, S. M., Skalak, T. C. and Rodeheaver, G. T. Ischemia-reperfusion injury in chronic pressure ulcer formation: A skin model in the rat. Wound Repair and Regeneration. 2000; 8: 68–76.

6. Black J, Baharestani M, Cuddigan J, Dorner B, Edsberg L, Langemo D, Posthauer. National Pressure Ulcer Advisory Panel's updated pressure ulcer staging system. Urol Nurs. 2007 Apr; 27(2):144-50, 156.

7. Sen, C. K. *et al*. Human skin wounds: a major and snowballing threat to public health and the economy. *Wound Repair Regen.* 2009; 17, 763–771.

8. NICE. Pressure ulcers: prevention and management of pressure ulcers. NICE clinical guideline. 2014.

9. Bennett G, Dealey C, Posnett J. The cost of pressure ulcers in the UK. Age Ageing. 2004 May;33(3):230-5.

10. David M. Studdert, L.L.B., Sc.D., Matthew J. Spittal, Ph.D., Michelle M. Mello,

J.D., Ph.D., A. James O'Malley, Ph.D., and David G. Stevenson, Ph.D. Relationship between Quality of Care and Negligence Litigation in Nursing Homes. N Engl J Med. 2011; 364:1243-1250.

11. Welton JM. Implications of Medicare reimbursement changes related to inpatient nursing care quality. J Nurs Adm. 2008 Jul-Aug;38(7-8):325-30.

12. Brown G. Long-term outcomes of full-thickness pressure ulcers: healing and mortality. Ostomy Wound Manage. 2003 Oct;49(10):42-50.

13. Gefen A, Farid KJ, Shaywitz I. A review of deep tissue injury development, detection, and prevention: shear savvy. Ostomy Wound Manage. 2013 Feb;59(2):26-35.

14. Susanne Colemana, Claudia Goreckia, E. Andrea Nelsonb, S. José Clossb, Tom Defloorc, Ruud Halfensd, Amanda Farrina, Julia Browna, Lisette Schoonhovene, Jane Nixona. International Journal of Nursing Studies. July 2013; Volume 50, Issue 7, Pages 974–1003.

15. Cho I, Noh M. Braden scale: Evaluation of clinical usefulness in an intensive care unit. J Adv Nurs. 2010;66(2):293–302.

16. Ayello, E. & Lyder, C. A new era of pressure ulcer accountability in acute care. *Adv. Skin Wound Care.* 2008; **21:**134–140

17. Norton L, Coutts P, Sibbald RG. Beds: practical pressure management for surfaces/mattresses. Adv Skin Wound Care. 2011 Jul;24(7):324-32.

18. Haugen V, Pechacek J, Maher T, Wilde J, Kula L, Powell J. Decreasing pressure ulcer risk during hospital procedures: a rapid process improvement workshop. J Wound Ostomy.2011 Mar-Apr;38(2):155-9.

19. Bethell E. Controversies in classifying and assessing grade 1 pressure ulcers. Nurs Times. 2003 Apr 1-7;99(13):73-5.

20. Fogerty MD, Abumrad NN, Nanney L, Arbogast PG, Poulose B, Barbul A. Risk factors for pressure ulcers in acute care hospitals. Wound Repair Regen. 2008 Jan-Feb;16(1):11-8.

21. Beeckman D, Schoonhoven L, Fletcher J, Furtado K, Gunningberg L, Heyman H,

Lindholm C, Paquay L, Verdu J, Defloor T. EPUAP classification system for pressure ulcers: European reliability study. J Adv Nurs. 2007; 60(6):682–691.

22. A. A. Weber, C. Gehin, G. Moddy, J. Jossinet, E. T. McAdams. Characterization of a multi-frequency wound impedance mapping instrument. Proceedings of the 30th IEEE EMBS Conference. 2008.

23. S. Treuillet, B. Albouy, and Y. Lucas. Three-dimensional assessment of skin wounds using standard digital camera. IEEE Trans. Med. Imaging. 2009; 28(5)752–762.

24. Deprez JF, Cloutier G, Schmitt C, Gehin C, Dittmar A, Basset O, Brusseau E. 3D ultrasound elastography for early detection of lesions evaluation on a pressure ulcer mimicking phantom. Conf Proc IEEE Eng Med Biol Soc. 2007; 2007:79-82.

25. Deprez JF, Brusseau E, Fromageau J, Cloutier G, Basset O. On the potential of ultrasound elastography for pressure ulcer early detection. Med Phys. 2011 Apr;38(4):1943-50.

26. Swisher SL, Lin MC2, Liao A2, Leeflang EJ3, Khan Y1, Pavinatto FJ1, Mann K1, Naujokas A4, Young D3, Roy S3, Harrison MR3, Arias AC1, Subramanian V1, Maharbiz MM5. Impedance sensing device enables early detection of pressure ulcers in vivo. Nat Commun. 2015 Mar 17;6:6575.

27. Francisco J. Veredas, Héctor Mesa, Laura Morente. Efficient detection of wound-bed and peripheral skin with statistical colour models. Medical & Biological Engineering & Computing. 2014.

28. Cula O, Dana K, Murphy F, Rao B. Skin texture modeling. Int J Comput Vis. 2005.

29. Jones TD, Plassmann P. An active contour model for measuring the area of leg ulcers. IEEE Trans Med Imaging. 2000; 19(12):1202–1210.

30. Qi H, Kong L, Wang C, Miao L. A hand-held mosaicked multispectral imaging device for early stage pressure ulcer detection. J Med Syst. 2011 Oct;35(5):895-904.

31. Rajendran PJ, Leachtenauer J, Kell S, Turner B, Newcomer C, Lyder C, Alwan M. Improving the detection of stage I pressure ulcers by enhancing digital color

images. Conf Proc IEEE Eng Med Biol Soc. 2006;1:5206-9.

32. Leachtenauer, J.C and Driggres. R.G. Surveillance and Reconnaissance Imaging Systems: Modeling and Performance Prediction. Artech House Boston MA. 2001; 228-241.

33. DaneshiKohan M, NasrAbadi A2. A temporal video-processing method to improve heart rate estimation. Perfusion. 2014.

34. Rosen J et al. Pressure ulcer prevention in black and white nursing home residents: A QI initiative of enhanced ability, incentives and management feedback. Advances in Skin and Wound Care. 2006;19:5, 262-268.

35. Nixon J et al. Skin alterations of intact skin and risk factors associated with pressure ulcer development in surgical patients: a cohort study. International Journal of Nursing Studies. 2007;44:5,655-663.

36. Brem H, Lyder C. Protocol for the successful treatment of pressure ulcers. Am J Surg. 2004.